

# Effects of vacancies on the properties of disordered ferroelectrics: A first-principles study

L. Bellaïche,<sup>1</sup> Jorge Íñiguez,<sup>2</sup> Eric Cockayne,<sup>3</sup> and B. P. Burton<sup>3</sup>

<sup>1</sup>*Physics Department, University of Arkansas, Fayetteville, Arkansas 72701, USA*

<sup>2</sup>*Institut de Ciència de Materials de Barcelona (ICMAB-CSIC), Campus de la UAB, 08193 Bellaterra (Barcelona), Spain*

<sup>3</sup>*Ceramics Division, Materials Science and Engineering Laboratory, National Institute of Standards and Technology, Gaithersburg, Maryland 20899-8520, USA*

(Received 8 September 2006; revised manuscript received 2 November 2006; published 22 January 2007)

A first-principles-based model is developed to investigate the influence of lead vacancies on the properties of the disordered  $\text{Pb}(\text{Sc}_{1/2}\text{Nb}_{1/2})\text{O}_3$  (PSN) ferroelectric. Lead vacancies generate large, inhomogeneous, electric fields that reduce barriers between energy minima for different polarization directions. This naturally explains why disordered ferroelectrics with significant lead vacancy concentrations have broadened dielectric peaks at lower temperatures, and why lead vacancies smear properties in the neighborhood of the ferroelectric transition in PSN. We also reconsider the conventional wisdom that lead vacancies reduce the magnitude of dielectric response.

DOI: [10.1103/PhysRevB.75.014111](https://doi.org/10.1103/PhysRevB.75.014111)

PACS number(s): 61.72.Bb, 61.43.-j, 61.72.Ji, 77.84.Dy

## I. INTRODUCTION

Experimentally, the introduction of vacancies into disordered ferroelectrics induces greater broadening of the dielectric response.<sup>1-3</sup> Other Pb-vacancy-induced effects include shifting of the dielectric peak to lower temperature; a decrease in the magnitude of the dielectric response; and a more “diffuse” phase transition.<sup>1-3</sup>

Defects are always present in real samples, and they often have a significant impact on measured properties, but the mechanisms responsible for vacancy-induced effects are mostly unknown. Understanding such mechanisms would illuminate the fundamentals of the behavior of disordered ferroelectrics, including those exhibiting the so-called *relaxor* features. One reason for this paucity of knowledge is that first-principles studies of (point) defects in ferroelectrics are scarce.<sup>4-7</sup>

Ultimately, one would like to study, via *ab initio* techniques, the effect(s) of Pb vacancies on the properties of disordered ferroelectrics exhibiting relaxor behavior, such as the prototype relaxor  $\text{Pb}(\text{Mg}_{1/3}\text{Nb}_{2/3})\text{O}_3$  (PMN). Unfortunately, because of the markedly different chemical character of Mg and Nb, PMN is a very challenging subject for *ab initio* modeling. Thus, in this manuscript we investigate instead the  $\text{Pb}(\text{Sc}_{1/2}\text{Nb}_{1/2})\text{O}_3$  (PSN) disordered ferroelectric, for which finite-temperature first-principles-based models are available.<sup>8,9</sup> Note that, unlike PMN which retains relaxor character down to 0 K (i.e., it exhibits no ferroelectric phase transition), chemically disordered PSN exhibits relaxor behavior between  $\sim 400$  K and  $\sim 368$  K, then transforms to a rhombohedral ferroelectric phase.<sup>1,2</sup> Interestingly, Ref. 1 reports that the introduction of 1.7% Pb vacancies into disordered PSN results in a  $\approx 2.6\%$  reduction of the  $T_m$  temperature at which the dielectric response is maximized (at low frequency), while smearing out the relaxor-to-ferroelectric transition. Furthermore, Ref. 2 indicates that lead vacancies can lead to the appearance of ferroelectricity at a slightly higher temperature than  $T_m$ .

Here we focus on static properties, because studying the dynamics of disordered ferroelectrics from first principles is

not currently feasible. Admittedly, this restriction, plus the close proximity of  $T_m$  to the ferroelectric transition temperature in PSN, makes it difficult to distinguish between effects of Pb vacancies that pertain specifically to relaxor characteristics, and those that pertain to disordered ferroelectrics in general. Therefore, we limit our conclusions to the effects of Pb vacancies on the properties of disordered ferroelectrics. Our study clarifies the origin(s) of the vacancy-induced effects mentioned above, and suggests that the common wisdom that Pb vacancies reduce the magnitude of dielectric response should be reconsidered.

This manuscript is organized as follows: Section II describes the method. Section III presents and discusses results. Section IV is a brief summary.

## II. METHOD

Our method is a generalization of the first-principles-derived effective Hamiltonian of Refs. 9–11 to investigate perovskites with chemical disorder on their  $B$  sites and Pb vacancies on their  $A$  sites, by writing the total energy as a sum of two terms:

$$E_{\text{PSN-DV}}(\{\mathbf{u}_i\}, \eta_H, \{\eta_j\}, \{\sigma_j\}, \{s_k\}) = E_{\text{PSN-D}}(\{\mathbf{u}_i\}, \eta_H, \{\eta_j\}, \{\sigma_j\}) + E_{\text{vac}}(\{\mathbf{u}_i\}, \{s_k\}), \quad (1)$$

where  $E_{\text{PSN-DV}}$  is the total energy of the  $\text{Pb}_{1-x}\square_x(\text{Sc}_{1/2}\text{Nb}_{1/2})\text{O}_3$  alloy (PSN-DV),  $\square$  representing a vacant  $A$  site;  $E_{\text{PSN-D}}$  is the total energy of chemically disordered PSN solid solutions (PSN-D);  $E_{\text{vac}}$  gathers the explicit energetics associated with Pb vacancies;  $\mathbf{u}_i$  is the ( $B$  centered) local polar distortion in unit cell  $i$  (proportional to the local dipole moment);  $\eta_H$  and  $\{\eta_j\}$  are the *homogeneous* and *inhomogeneous* strain tensors,<sup>12</sup> respectively;  $\sigma_j = -1$  or  $+1$  if there is a Sc or Nb cation, respectively, at the  $B$ -lattice site  $j$  of the  $\text{Pb}_{1-x}\square_x(\text{Sc}_{1/2}\text{Nb}_{1/2})\text{O}_3$  alloy. Finally,  $\{s_k\}$  characterizes the amount and distribution of  $A$ -site vacancies, i.e.,  $s_k = 0$  or  $1$  if the  $k$ 'th  $A$  site is occupied by a lead atom or vacant, respectively.

For  $E_{\text{PSN-D}}$ , we use the analytical expression proposed in Ref. 9, which includes a term of the form  $-\sum_i Z^* \mathbf{u}_i \cdot \boldsymbol{\epsilon}_i \{\sigma_j\}$ ,

where  $Z^*$  is the Born effective charge associated with the local distortion, and  $\epsilon_i$  is the internal field at cell  $i$  that is caused by the surrounding  $B$ -site cation distribution.<sup>13</sup>

For  $E_{\text{vac}}$ , we use the following perturbative expression (first order in  $\mathbf{u}_i$ ):

$$E_{\text{vac}}(\{\mathbf{u}_i\}, \{s_{kj}\}) = \sum_k \sum_i S_{k,i} s_{kj} \mathbf{g}_{ki} \cdot \mathbf{u}_i, \quad (2)$$

where the sum over  $k$  runs over  $A$  sites, and the sum over  $i$  runs over  $B$  sites. The  $S_{k,i}$  parameters quantify how vacancies perturb the local distortions.  $\mathbf{g}_{ki}$  is the unit vector joining the  $A$  site  $k$  to the  $B$ -site-center of  $\mathbf{u}_i$ . We truncated  $S_{k,i}$  at the first-neighbor shell. All the parameters of Eqs. (1) and (2) are derived from first-principles calculations<sup>14–16</sup> performed on relatively small supercells (i.e., up to 40 atoms), including one (to obtain  $S_{k,i}$ ) that exhibits a lead vacancy and a background charge of  $-2$ .

We solve this effective Hamiltonian by the Monte Carlo (MC) technique<sup>17</sup> to simulate properties of two different systems: (i) disordered  $\text{Pb}(\text{Sc}_{1/2}\text{Nb}_{1/2})\text{O}_3$  without any Pb vacancies, PSN-D; (ii) disordered  $\text{Pb}_{0.95}\square_{0.05}(\text{Sc}_{1/2}\text{Nb}_{1/2})\text{O}_3$ , PSN-DV, which has a realistic 5% vacancy concentration on its  $A$  sites<sup>1,2</sup>. A  $12 \times 12 \times 12$  supercell (8640 atoms, 48 Å lateral size) is used for both systems. The variables  $\sigma_j$  and  $s_k$  are randomly chosen, and remain constant during the simulation. Temperature  $T$  is decreased in small steps from high  $T$ . We found it unusually difficult to get good statistics and, therefore, performed 10 MC runs of 4 million sweeps each, at every temperature. We collect the supercell average  $\mathbf{u}$  of the local distortion at each sweep and classify it as *visiting* one of the eight rhombohedral, twelve orthorhombic, or six tetragonal energy minima by computing its projection onto each of these twenty-six high-symmetry directions. The *visiting rate* of a particular minimum is defined as the ratio between the number of sweeps in which that minimum is visited and the total number of sweeps. The  $\chi_{\alpha\beta}$  dielectric susceptibility tensor is computed as in Refs. 18 and 19, that is by using the polarization fluctuation formula:

$$\chi_{\alpha\beta} = \frac{(NZ^*)^2}{V\epsilon_0 k_B T} [\langle u_\alpha u_\beta \rangle - \langle u_\alpha \rangle \langle u_\beta \rangle] \quad (3)$$

where  $\langle u_\alpha u_\beta \rangle$  denotes the statistical average of the product between the  $\alpha$  and  $\beta$  components of the supercell average of the local mode vectors, and where  $\langle u_\alpha \rangle$  (respectively,  $\langle u_\beta \rangle$ ) is the statistical average of the  $\alpha$ - (respectively,  $\beta$ -) component of the supercell average of the local mode vectors.  $N$  is the number of sites in the supercell while  $V$  is its volume.  $k_B$  is the Boltzmann's constant and  $\epsilon_0$  is the permittivity of the vacuum. Note that a detailed derivation of Eq. (3) is provided in Ref. 19.

### III. RESULTS

The simulated temperature at which the dielectric response is maximized,  $T_m$ , is about 850 K for PSN-D and 794 K for PSN-DV.<sup>20</sup> Thus, our model qualitatively reproduces the previous finding that Pb vacancies reduce  $T_m$ .<sup>1,2,6</sup> Our quantitative prediction of a 6.5% reduction in  $T_m$ , from

the introduction of 5% Pb vacancies agrees rather well with the corresponding experimental reduction of 8.5%,<sup>2</sup> and is also consistent with the  $\approx 2.6\%$  reduction of  $T_m$  associated with 1.7% Pb vacancies;<sup>1</sup> establishing the accuracy of simulations based on Eqs. (1) and (2). Note that Eq. (2) can be rewritten as  $E_{\text{vac}}(\{\mathbf{u}_i\}, \{s_{kj}\}) = -\sum_i Z^* \mathbf{u}_i \cdot \epsilon_{\text{vac},i}[\{s_{kj}\}]$ , with  $\epsilon_{\text{vac},i} = -\frac{1}{Z^*} \sum_k S_{k,i} s_{kj} \mathbf{g}_{ki}$ ; that is,  $\epsilon_{\text{vac},i}$  has the dimensions and physical meaning of an internal electric field arising from the Pb vacancies. Our first-principles-derived values for the fields around a Pb vacancy are of the order of  $1.4 \times 10^9$  V/m at each neighboring  $B$  site  $i$ . These fields are oriented towards the vacancy because  $S_{k,i}$  is positive and  $\epsilon_{\text{vac},i}$  depends on the directional  $\mathbf{g}_{ki}$  vectors;  $\epsilon_{\text{vac},i}$  is therefore rather large and *inhomogeneous*, and thus significantly *opposes* homogeneous ferroelectric  $\{\mathbf{u}_i\}$  ordering, which explains the vacancy-induced reduction of  $T_m$ .

Figure 1(a) displays the  $(u_x, u_y, u_z)$  supercell averages of local distortions as functions of the reduced temperature  $T/T_m$ ;  $(u_x, u_y, u_z)$  is directly proportional to the spontaneous polarization, where the  $x$ ,  $y$ , and  $z$  axes are chosen along the pseudocubic [100], [010], and [001] directions, respectively]. Both PSN-D and PSN-DV are predicted to have a low- $T$  rhombohedral ferroelectric phase in which  $u_x \approx u_y \approx u_z$ , in agreement with experiment.<sup>1,2</sup> Therefore, only the average component,  $\langle \bar{u} \rangle = 1/3 \langle u_x + u_y + u_z \rangle$ , is plotted in Fig. 1(a). Also shown in Fig. 1(a) is  $\langle |u| \rangle_R / \sqrt{3}$ , where  $\langle |u| \rangle_R$  is the mean *magnitude* of the supercell average of local distortions calculated from sweeps in which the system visits rhombohedral minima. Figure 1(b) shows  $\chi$ —which corresponds to one third of the trace of the  $\chi_{\alpha\beta}$  dielectric susceptibility tensor—versus  $T/T_m$ . In other words, and according to Eq. (3) and the definition of  $\chi$ , Fig. 1(b) displays

$$\chi = \frac{(NZ^*)^2}{V\epsilon_0 k_B T} \frac{1}{3} [\langle u_x^2 + u_y^2 + u_z^2 \rangle - (\langle u_x \rangle^2 + \langle u_y \rangle^2 + \langle u_z \rangle^2)]. \quad (4)$$

Predictions for  $\langle \bar{u} \rangle$  and  $\chi$  are quite scattered around  $T_m$ , which reflects our difficulties in obtaining good statistics for either PSN-D or PSN-DV, as expected for systems with complex energy landscapes.<sup>22</sup> We smoothed the results for  $\langle \bar{u} \rangle$  by fitting them to a 7th-order polynomial in the region around  $T_m$  [lines in Fig. 1(a)]. We denote the result by  $\langle \bar{u} \rangle_{\text{fit}}$  and recompute the susceptibility as

$$\chi_{\text{fit}} = \frac{N(Z^*)^2}{a_0^3 \epsilon_0 k_B T} \left( \frac{1}{3} \langle |u| \rangle_R^2 - \langle \bar{u} \rangle_{\text{fit}}^2 \right), \quad (5)$$

where  $a_0$  is the 0 K cubic lattice constant. We obtain Eq. (5) from Eq. (4), by approximating  $V$  as  $Na_0^3$ , and the averages as follows:  $1/3 \langle u_x^2 + u_y^2 + u_z^2 \rangle \sim 1/3 \langle |u| \rangle_R^2$  and  $1/3 (\langle u_x \rangle^2 + \langle u_y \rangle^2 + \langle u_z \rangle^2) \sim \langle \bar{u} \rangle_{\text{fit}}^2$ .<sup>23</sup> The “smoothed”  $\chi_{\text{fit}}$ 's are depicted with lines in Fig. 1(b), and will be used in combination with  $\langle \bar{u} \rangle_{\text{fit}}$ , to illuminate the effects of Pb vacancies in disordered ferroelectrics.

Interestingly, Fig. 1(b) indicates that, contrary to common wisdom and previously reported observations,<sup>1,2</sup> our predicted maximum value of the dielectric response does *not* decrease when Pb vacancies are introduced: our simulations

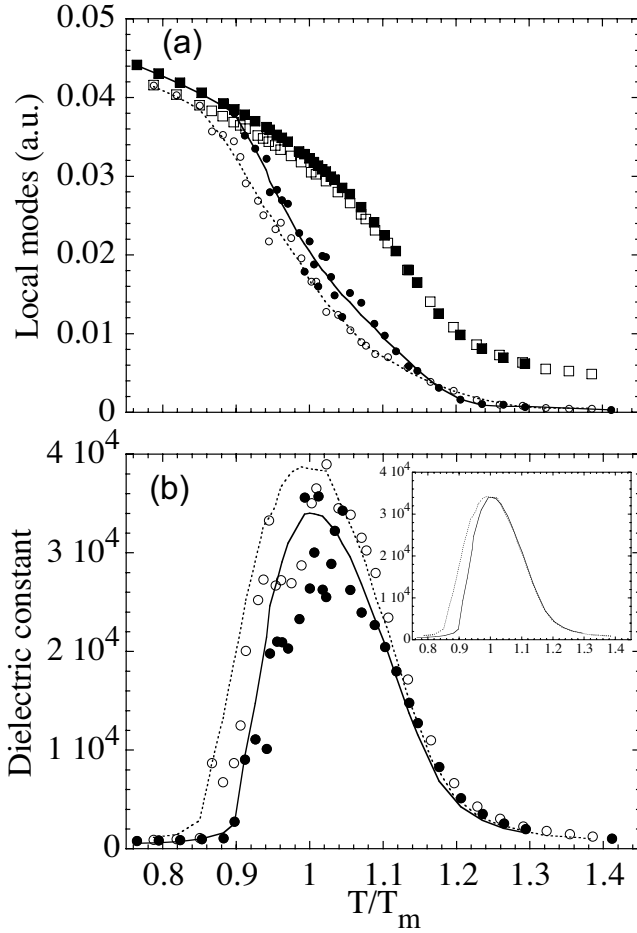


FIG. 1. Properties of PSN-DV (open dots, dashed lines) and PSN-D (filled dots, solid lines) as functions of  $T/T_m$ . Dots in panel (a) show the supercell-averaged mean component of the local distortions ( $\langle \bar{u} \rangle$ ). Lines represent fits to a 7th order polynomial ( $\langle \bar{u} \rangle_{\text{fit}}$ ). In panel (a), we also show (squares) the magnitudes of the local distortions,  $\langle |u| \rangle_R$ , divided by  $\sqrt{3}$ . Panel (b) displays one third of the trace of the dielectric susceptibility tensor directly obtained from MC simulations. The lines represent the  $\chi_{\text{fit}}$  results obtained from Eq. (5). The inset of panel (b) displays  $\chi_{\text{fit}}$  results that were rescaled to match  $\chi_{\text{fit}}$  of PSN-D at  $T=T_m$ .

indicate that  $\chi_{\text{fit}}$  is slightly larger in PSN-DV than in PSN-D at  $T=T_m$ , because  $T_m$  is smaller and  $\langle \bar{u} \rangle_{\text{fit}}$  is further away from  $\langle |u| \rangle_R / \sqrt{3}$  in PSN-DV, see Fig. 1(a) and Eq. (5). [Our predicted maximum values for  $\chi_{\text{fit}}$  are about 34 000 and 38 500 for PSN-D and PSN-DV, respectively, which is close to the measured value  $\approx 40\,000$  of Ref. 1 for PSN-D]. This result, which appears to be at odds with measurements, is explained by the experimental observation of Ref. 24 that Pb vacancies in  $\text{Pb}(\text{Sc}_{1/2}\text{Nb}_{1/2})\text{O}_3$  favor the simultaneous formation of pyrochlore phases ( $\text{Pb}_{2.31}\text{Nb}_2\text{O}_{7.31}$  and  $\text{Pb}_3\text{Nb}_4\text{O}_{13}$ ). Thus, dielectric measurements on a PSN-DV sample at  $T=T_m$  should yield a *smaller* response than those on PSN-D; because, while the majority of the PSN-DV sample is perovskite, with a dielectric response that is at least as large as that for PSN-D, a smaller fraction is pyrochlore, which has a much *smaller* dielectric response.<sup>24</sup>

Figure 1(b) also shows that our simulations successfully

TABLE I. Total energy per five-atom cell  $E$ , at 5 K, and visiting rate  $v_r$  at  $T/T_m \approx 0.93$  associated with the different rhombohedral  $\langle 111 \rangle$  and orthorhombic  $\langle 110 \rangle$  minima in PSN-D and PSN-DV. The zero of energy corresponds to the ground state. The uncertainty is lower than 0.01 meV and 0.1% for  $E$  and  $v_r$ , respectively.

Minimum	$E$ (meV) in PSN-D	$E$ (meV) in PSN-DV	$v_r$ in PSN-D (%)	$v_r$ in PSN-DV (%)
[-1-11]	0.38	0.41	6.3	0.0
[-111]	0.00	0.23	72.9	0.0
[111]	0.07	0.00	20.0	0.0
[1-11]	0.68	0.58	0.0	0.0
[1-1-1]	0.00	0.28	0.0	37.2
[11-1]	0.67	0.33	0.0	17.3
[-11-1]	0.65	0.38	0.0	5.8
[-1-1-1]	0.20	0.32	0.0	37.5
[-101]	3.05	2.90	0.3	0.0
[011]	3.05	2.80	0.5	0.0
[101]	3.45	2.85	0.0	0.0
[1-10]	3.42	3.42	0.0	0.0
[10-1]	3.48	2.93	0.0	0.7
[01-1]	3.85	2.99	0.0	0.2
[-10-1]	3.60	3.12	0.0	0.2
[0-1-1]	3.05	2.85	0.0	1.1
[0-11]	3.71	3.29	0.0	0.0
[110]	3.69	3.34	0.0	0.0
[-110]	3.54	3.31	0.0	0.0
[-1-10]	3.58	3.53	0.0	0.0

reproduce two experimental observations: (i) the *broadened* dielectric peaks in PSN-D and PSN-DV, which, according to Eq. (5) and Fig 1(a), arise from the diffuse phase transition associated with  $\langle \bar{u} \rangle_{\text{fit}}$ ; (ii) Pb vacancy-induced dielectric *broadening*.<sup>1-3</sup> Half-maximum width of the  $\chi_{\text{fit}}$  peak is about 0.19 in PSN-D versus 0.22 in PSN-DV (in reduced units) [c.f. the corresponding predicted value of 0.13 reported in Ref. 25 for the “normal” ferroelectric system  $\text{Pb}(\text{Zr}_{0.6}\text{Ti}_{0.4})\text{O}_3$ ]. Note that vacancy-induced dielectric broadening only occurs *below*  $T_m$ . This is particularly clear in the Fig. 1(b) inset, in which the  $\chi_{\text{fit}}$  of PSN-DV is rescaled by a  $T$ -independent constant to match the  $\chi_{\text{fit}}$  dielectric response of PSN-D at  $T=T_m$ .

To clarify how PSN-DV differs from PSN-D only at temperatures below  $T_m$ , Table I lists the internal energies of rhombohedral and orthorhombic minima (calculated at 5 K); plus the visiting rates of these minima in both PSN-D and PSN-DV at  $T/T_m \approx 0.93$ . The energy landscape of PSN-D is rather anisotropic; e.g., the energy difference between the ground state and the highest-lying rhombohedral minimum is 0.68 meV. Reference 25 demonstrated that such local symmetry breaking is caused by the anisotropy of the large internal  $\epsilon_r$  electric fields (which have an average magnitude  $\approx 2 \times 10^9$  V/m; determined numerically) that arise from the charge-difference between  $\text{Sc}^{3+}$  and  $\text{Nb}^{5+}$  ions. This anisotropy results from our nanometric periodic PSN-D supercell

being too small to contain a perfectly random  $B$ -site configuration.<sup>25</sup> Results in Table I also indicate that, at  $T/T_m \approx 0.93$ , PSN-D preferentially visits the rhombohedral  $[-111]$  and  $[111]$  minima, i.e., the minima that have *lowest* energies, and that are connected by one of the lowest-in-energy orthorhombic minima (specifically,  $[011]$ ). Such fluctuations lead to a  $\langle \bar{u} \rangle_{\text{fit}}$  that is smaller than  $\langle |u| \rangle_R / \sqrt{3}$ , and thus [Eq. (5)], to a large dielectric response relative to normal ferroelectrics [which are already stuck in a single minimum at  $T/T_m \approx 0.93$  (Ref. 25)]. As indicated by Table I, the  $\epsilon_{\text{vac},i}$  electric field associated with Pb vacancies [see rewriting of Eq. (2) above] brings the orthorhombic and rhombohedral minima closer to each other; similar to the finding of Ref. 25 that  $\epsilon_i$  in PSN-D reduces barriers between energy minima. Thus, PSN-DV fluctuates more and/or visits more minima than PSN-D at temperatures below  $T_m$ . This implies a smaller  $\langle \bar{u} \rangle_{\text{fit}}$  [Fig. 1(a)] and therefore naturally explains two vacancy-induced effects that have been observed experimentally:<sup>1-3</sup> a broader PSN-DV dielectric response [Fig. 1(b) and Eq. (5)]; and a more diffuse PSN-DV phase transition [PSN-DV “only” begins to stick in a single rhombohedral minimum at  $T/T_m \approx 0.85$  as indicated by the equality  $\langle \bar{u} \rangle_{\text{fit}} = \langle |u| \rangle_R / \sqrt{3}$  at and below this temperature, Fig. 1(a), whereas, freezing in of PSN-D occurs at  $T/T_m \approx 0.90$ ].

Results in Table I also indicate that the most frequently visited rhombohedral minima in PSN-DV are *not* the lowest-energy minima; rather they are those with small-in-energy rhombohedral-to-orthorhombic barriers (e.g., the  $[1-1-1]$  and  $[-1-1-1]$  minima that are connected by the  $[0-1-1]$  minimum, over an energy barrier of about 2.5 meV). This strongly suggests that disordered ferroelectrics with Pb vacancies can be thought of as nonergodic systems.<sup>26</sup>

#### IV. SUMMARY

In summary, first-principles-based calculations predict that the introduction of Pb vacancies in  $\text{Pb}(\text{Sc}_{1/2}\text{Nb}_{1/2})\text{O}_3$  (i) reduces the temperature at which the dielectric response peaks,  $T_m$ , consistent with experiment;<sup>1-3</sup> (ii) does *not intrinsically* decrease the magnitude of the dielectric peak, contrary to common wisdom;<sup>1-3</sup> (iii) broadens the dielectric response and enhances the diffuse character of the ferroelectric transition, consistent with measurements<sup>1-3</sup> (but only at temperatures below  $T_m$ ). Item (i) above is the direct consequence of the relatively large internal inhomogeneous electric fields generated by the Pb vacancies. We suggest that our disagreement with experiments in item (ii) is caused by parasitic pyrochlore phases in the experimental samples. Item (iii) originates from the decrease in energy barriers that are caused by Pb vacancies, which promote enhanced fluctuations between different energy minima below  $T_m$ . Interestingly, our results regarding the effect of defects on energy landscape may also be relevant for modeling (and understanding) *dynamical* properties of disordered ferroelectrics.

#### ACKNOWLEDGMENT

We thank J. M. Kiat, B. Dkhil, and C. Malibert for useful discussions. This work is supported by ONR Grant Nos. N00014-01-1-0365, N00014-04-1-0413, and N00014-01-1-0600, by NSF Grant No. DMR-0404335, and by DOE Grant No. DE-FG02-05ER46188. J.I. thanks financial support from the Spanish Ministry of Science and Education (“Ramón y Cajal” program and Grant No. BFM2003-03372-C03-01), the Catalan Government Grant No. SGR-2005-683, and FAME-NoE.

<sup>1</sup>F. Chu, I. M. Reaney, and N. Setter, *J. Appl. Phys.* **77**, 1671 (1995).

<sup>2</sup>C. Malibert, B. Dkhil, J. M. Kiat, D. Durand, J. F. Berar, and A. Spasojevic-de Bire, *J. Phys.: Condens. Matter* **9**, 7485 (1997).

<sup>3</sup>F. Chu, N. Setter, and A. K. Tagantsev, *J. Appl. Phys.* **74**, 5129 (1993).

<sup>4</sup>E. Cockayne and B. P. Burton, *Phys. Rev. B* **69**, 144116 (2004).

<sup>5</sup>S. Poykko and D. J. Chadi, *Phys. Rev. Lett.* **83**, 1231 (1999).

<sup>6</sup>B. P. Burton, E. Cockayne, S. Tinte, and U. V. Waghmare, *Phase Transitions* **79**, 91 (2006).

<sup>7</sup>H. Crogman and L. Bellaiche, *Phys. Rev. B* **66**, 220103(R) (2002).

<sup>8</sup>B. P. Burton, E. Cockayne, and U. V. Waghmare, *Phys. Rev. B* **72**, 064113 (2005).

<sup>9</sup>R. Hemphill, L. Bellaiche, A. García, and D. Vanderbilt, *Appl. Phys. Lett.* **77**, 3642 (2000).

<sup>10</sup>L. Bellaiche, A. García, and D. Vanderbilt, *Phys. Rev. Lett.* **84**, 5427 (2000).

<sup>11</sup>L. Bellaiche, A. García, and D. Vanderbilt, *Ferroelectrics* **266**, 41 (2002).

<sup>12</sup>W. Zhong, D. Vanderbilt, and K. M. Rabe, *Phys. Rev. Lett.* **73**, 1861 (1994); *Phys. Rev. B* **52**, 6301 (1995).

<sup>13</sup>A. M. George, J. Íñiguez, and L. Bellaiche, *Nature (London)* **413**, 54 (2001); J. Íñiguez and L. Bellaiche, *Phys. Rev. Lett.* **87**, 095503 (2001).

<sup>14</sup>D. Vanderbilt, *Phys. Rev. B* **41**, 7892 (1990).

<sup>15</sup>P. Hohenberg and W. Kohn, *Phys. Rev.* **136**, B864 (1964); W. Kohn and L. J. Sham, *ibid.* **140**, A1133 (1965).

<sup>16</sup>L. Bellaiche and D. Vanderbilt, *Phys. Rev. B* **61**, 7877 (2000).

<sup>17</sup>N. Metropolis, A. W. Rosenbluth, M. N. Rosenbluth, A. H. Teller, and E. Teller, *J. Chem. Phys.* **21**, 1087 (1953).

<sup>18</sup>A. García and D. Vanderbilt, in *First-Principles Calculations for Ferroelectrics: Fifth Williamsburg Workshop*, edited by R. E. Cohen (AIP, Woodbury, NY, 1998), p. 53; *Appl. Phys. Lett.* **72**, 2981 (1998).

<sup>19</sup>K. M. Rabe and E. Cockayne in *First-Principles Calculations for Ferroelectrics: Fifth Williamsburg Workshop*. (Ref. 18), p. 61.

<sup>20</sup>Note that the experimental values of  $T_m$  are lower than our predictions, e.g., the observed temperature is  $\sim 380$  K in PSN-D. (Refs. 1 and 2) Preliminary results [derived from the development of a numerical scheme incorporating ferroelectric *and* antiferrodistortive degrees of freedom in the effective Hamiltonian scheme (Ref. 21)] strongly suggest that this discrepancy is due to the neglect of oxygen-octahedra rotation in our models.

- <sup>21</sup>I. A. Kornev, L. Bellaiche, P.-E. Janolin, B. Dkhil, and E. Suard, Phys. Rev. Lett. **97**, 157601 (2006).
- <sup>22</sup>D. Viehland, S. J. Jang, L. E. Cross, and M. Wuttig, J. Appl. Phys. **68**, 2916 (1990); Phys. Rev. B **46**, 8003 (1992).
- <sup>23</sup>Note that we numerically checked that (i)  $1/3\langle u_x^2 + u_y^2 + u_z^2 \rangle$  is very well approximated by  $1/3\langle |u|_R^2 \rangle$ ; (ii)  $1/3(\langle u_x \rangle^2 + \langle u_y \rangle^2 + \langle u_z \rangle^2)$  is also well approximated by  $\langle \vec{u} \rangle_{\text{fit}}^2$ ; and (iii) the polarization fluctuation formula [see Eq. (3)] provides the same dielectric constant as the one (directly) obtained by computing the electric-field-induced change in polarization.
- <sup>24</sup>F. Guibert, thesis, Université Paris-Sud XI, 2002.
- <sup>25</sup>J. Íñiguez and L. Bellaiche, Phys. Rev. B **73**, 144109 (2006).
- <sup>26</sup>I. A. Kornev and L. Bellaiche, Phys. Rev. Lett. **91**, 116103 (2003).